Preprints of the 21st IFAC World Congress (Virtual)
Berlin, Germany, July 12-17, 2020

Adaptive Artificial Potential Fields with Orientation Control Applied to Robotic Manipulators

Caio Cristiano Barros Viturino *
Ubiratan de Melo Pinto Junior *
André Gustavo Scolari Conceição * **Leizer Schnitman** **

* *LaR - Robotics Laboratory, Department of Electrical and Computer Engineering, Federal University of Bahia, Salvador, Brazil. E-mails: engcaiobarros@gmail.com, eng.ele.ubiratan@gmail.com, andre.gustavo@ufba.br*
** *CTAI - Training Center in Technology in Industrial Automation , Department of Chemical Engineering, Federal University of Bahia, Salvador, Brazil. E-mail: leizer@ufba.br*

Abstract: This paper proposes the integration of an Adaptive Artificial Potential Fields algorithm with a new end effector orientation control technique for real-time robot path planning. The development of autonomous robotic systems has undergone several advances in path planning algorithms. These systems generate object collision-free paths in the robot's workspace. In this context, the Artificial Potential Fields technique has been the focus of improvements in recent years due to its simplicity of application and efficiency in real-time systems, since it does not require a global mapping of the robot's workspace. In spite of its efficiency, this technique is susceptible to local minimum problems of different natures, such as *Goals Non-Reachable with Obstacles Nearby* (GNRON). To solve this problem, we suggest the use of an improvement called Adaptive Artificial Potential Fields used in conjunction with the proposed end effector orientation control technique, which allows reaching a desired orientation of the end effector. The resulting force, generated from the Adaptive Artificial Potential Field, guides the robot end effector to the goal. The *Robot Operating System* (ROS) framework and a collaborative robot manipulator UR5 are used to validate the proposed method on an approaching task for an object on a 3D printer tray.

Keywords: Artificial Potential Field, Orientation Control, Robotic manipulators, Path planning

1. INTRODUCTION

Technological developments allow new generations of robots to become increasingly autonomous. In this respect, robots may have abilities of perception, location, control, and self-decision (Leite et al., 2015). One of the goals of autonomous robotic systems is to perform a secure control of movement so that there is no collision with obstacles such as people, machines and objects (Thomas et al., 2011). This objective requires treatment of various problems such as location, movement control, as well as trajectory and path planning.

An example of a path planning algorithm for real-time application of an anti-collision system in manipulating and mobile robots, known as Artificial Potential Fields (APF), was firstly proposed by Khatib (1986). With the use of APFs in manipulator robots, the links are seen as charged particles that undergo intervention of repulsive potential fields generated by obstacles and an attractive field generated by the final, or objective, position. Despite their efficiency, classical APFs have some restrictions or local minimum, such as:

- Inability to reach a desired end effector orientation in case of robot manipulators.
- Failure to achieve the goal when it is within the obstacle's influence area, a problem known as *Goals Non-Reachable with Obstacles Nearby* (GNRON) (Ge and Cui, 2000). This problem occurs in mobile and manipulator robots.
- Non-convergence of the path in the positioning configurations where there are obstacles near the links. The obstacle's repulsive forces prevent the end effector from reaching the goal, problem known as Reacharound Local Minimum Problem (RLMP) (Byrne et al., 2013). This problem occurs exclusively in robotic manipulators.
- The generated path need post-processing in order to make it smoother.

The increasing research in the area of collision avoidance using the APF method has been remarkable due to its typically small computation times (Quiroz-Omaña and Adorno, 2019). The application areas include manipulator robots, mobile robots, autonomous cars, unmanned aerial vehicles (UAVs), autonomous underwater vehicles, among others. Some works in the area, as proposed by Ge and Cui

(2000), developed a technique called Modified Artificial Potential Fields (MAPF) to solve GNRON problems in mobile robots. An expansion to a three-dimensional space of this technique was presented by Luo et al. (2012), but increasing the chances of stagnation in a local minimum. Zhang et al. (2017) developed the so-called Adaptive Artificial Potential Fields (AAPFs) to solve this MAPF's problem. In this method, concepts of classical APFs are used, when distant from the objective, and MAPFs, when it is close to the objective. Thus, the path travelled does not face problems related to local minimum caused by the repulsive potential fields and, at the same time, is able to solve the GNRON problem.

The integration of classic APFs into Collision Cone Approach was proposed by Kim et al. (2016), so that a possible collision between mobile robots and obstacles can be predicted. Li et al. (2015) presented a method of path planning for mobile robots in known, partially known or totally unknown environments. The APFs were integrated into the *Simultaneous Forward Search Method* (SIFORS) to find a valid and short path to the objective.

APFs have some local minimum problems specific of mobile and manipulators robots. Mobile robots have greater freedom of movement, whereas in a chain of rigid bodies of a manipulator, the movement of each joint changes the position of the previous joint to reach a goal determined by the path planning algorithm. When attempting to reach a final position, a robotic manipulator may stagnate to a local minimum due to the repulsive forces acting on the links, a problem known as RLMP. Byrne et al. (2013) used the methods known as *Goal Configuration Sampling*, *Subgoal-Selection*, based on the *Sampling-based* method and the *Expanded Convex Hull* algorithm, to avoid RLMPs local minimum caused by APFs. Akbaripour and Masehian (2017) developed a method that integrates *Probabilistic Roadmap Method* (PRM) and *Lazy-PRM* algorithms. This method was named Semi-Lazy Probabilistic Roadmap Method (SLPRM) and it is based on Sampling-based algorithms. The method was developed for application in robot manipulators. The results showed that the computational efficiency of the *SLPRM* algorithm is higher when compared to the PRM and the *Lazy-PRM* algorithms.

Orientation control plays a key role in path planning. The end effector is sometimes required to be in a specific orientation in order to pass in narrow passages. The APF method itself does not provide orientation control. That is, it is not possible to set a goal orientation using only the APF classic method. To solve this problem, this paper presents a new approach to path planning, where AAPF is used with an end effector orientation control technique. It was also shown that the AAPF method reduces the jitter by allowing robot joints to smoothly enter the area of influence of obstacles. This is not the desired behaviour except for the end effector. Due to this, the AAPF method was only applied to the end effector while the APF method was applied to all other joints. Experimental results demonstrate the performance of the proposed approach to solve GNRON problem and orientation control.

The paper is organized as follows. Section 2 shows the theory of classical APFs. Section 3 deals with AAPF as a solution to the GNRON problem. Section 4 shows our proposed end effector orientation control technique using AAPF. Section 5 shows the experimental results discussing the advantages of the use of the end effector orientation control technique with the AAPF in typical advanced manufacture approach applications. Section 6 concludes the article and discusses suggestions for future work.

2. CLASSIC ARTIFICIAL POTENTIAL FIELDS

In classic APF method, the expression of the attractive potential function is

$$U_{att}(q) = \frac{1}{2}\zeta\rho^2 \tag{1}$$

where ζ is a parameter used as an attractive field scale factor.

The repulsive field is nullified after a certain distance of influence ρ_0 from the obstacle and raises it when close to it, that is,

$$U_{rep}(q) = \begin{cases} \frac{1}{2}\eta_j \left(\frac{1}{\rho} - \frac{1}{\rho_0}\right)^2 & ; \quad \rho \leq \rho_0 \\ 0 & ; \quad \rho > \rho_0 \end{cases} \tag{2}$$

where the obstacle influence distance is represented by ρ_0, the smallest distance of q to the boundaries of an obstacle in the configuration space is defined by ρ and η_j is a gain coefficient that determines the influence of the repulsive field.

Attractive and repulsive fields resemble the concept of electrostatic fields. The force acting on the robot is equivalent to the negative gradient of U and is given by:

$$F(q) = -\nabla U(q) = -\nabla U_{att}(q) - \nabla U_{rep}(q) \tag{3}$$

One of the requirements to be considered by the attractive potential field is to increase with the distance between q_{end} and $q_{initial}$. In order to avoid discontinuities in attractive forces, APF uses a quadratically growing field with the distance of q_{final}. Where ρ_f is the Euclidean distance between q and q_{final}, denoted by:

$$\rho_f(q) = ||q - q_{final}|| \tag{4}$$

It is possible to set the quadratic attractive field to $\nabla U_{att}(q)$ such that

$$\nabla U_{att}(q) = \nabla \frac{1}{2}\zeta\rho_f^2(q) = \zeta(q - qfinal) \tag{5}$$

For the parabolic well, the attractive force, $F_{att}(q) = -\nabla U_{att}(q)$ is a vector directed toward q_{final}.

The expression for repulsive force is:

$$F_{rep}(q) = \begin{cases} \eta_j \left(\frac{1}{\rho} - \frac{1}{\rho_0}\right) \frac{1}{\rho^2} \nabla\rho & ; \quad \rho \leq \rho_0 \\ 0 & ; \quad \rho > \rho_0 \end{cases} \tag{6}$$

where $\nabla\rho$ indicates the gradient $\nabla\rho(x)$ evaluated at $x = C_j(q)$. If a b point in the obstacle boundary in the workspace is close to the repulsive field of a control point

in the robot, then $\nabla\rho = ||c_j(q) - b||$ and its gradient is represented by:

$$\nabla\rho(x)\big|_x = \frac{a_j(q) - b}{||a_j(q) - b||} \tag{7}$$

The forces acting on the robot are summed and applied to each joint i through the transposed Jacobian to obtain the necessary torque to move the joints. The total artificial joint torque acting on the arm is defined as:

$$\tau(q) = \sum_i J_i^T(q) F_{att,i}(q) + \sum_i J_i^T(q) F_{rep,i}(q) \tag{8}$$

3. ADAPTATIVE ARTIFICIAL POTENTIAL FIELDS

To eliminate GNRON problems present in classical APFs, Zhang et al. (2017) developed the AAPF. The repulsive field of AAPFs is represented by

$$U_{rep}(q) = \begin{cases} \frac{1}{2}\eta_j \left(\frac{1}{\rho} - \frac{1}{\rho_0}\right)^2 \frac{\rho_g^n}{1+\rho_g^n} & ; \quad \rho \le \rho_0 \\ 0 & ; \quad \rho > \rho_0 \end{cases} \tag{9}$$

where ρ_g is the distance from the joint to the goal and $n > 0$.

In (9), when $n = 1$ and the robot is far from the target, that is, $\rho_g^n \gg 1$, then $\rho_g^n/(1\rho_g^n) \approx 1$ and the repulsive fields of AAPFs are equivalent to the repulsive fields of APFs, avoiding the path from increasing as the distance to the target increases. When the robot is near the goal, i.e. $\rho_g^n \ll 1$, the expression $\rho_g^n/(1\rho_g^n)$ is equivalent to approximately ρ_g.

In AAPF, the repulsive force is fragmented into two other components, which draw the robot to the target and repel it from the obstacle even though it is positioned within the area of influence ρ_0, that is,

$$F_{rep}(q) = \begin{cases} F_{rep1}\ \gamma_{OR} + F_{rep2}\ \gamma_{RG} & ; \quad \rho \le \rho_0 \\ 0 & ; \quad \rho > \rho_0 \end{cases} \tag{10}$$

where the unit vector $\gamma_{OR} = \nabla\rho(q, q_{obs})$ indicates the direction from the obstacle to the robot control point and $\gamma_{RG} = -\nabla\rho(q, q_{goal})$ indicates the robot's direction to the goal.

The F_{rep1} component, represented by:

$$F_{rep1} = \eta_j \left(\frac{1}{\rho} - \frac{1}{\rho_0}\right) \frac{\rho_g^n}{\rho^2(1+\rho_g^n)} \tag{11}$$

repels robot from the obstacle and the F_{rep2} component, represented by:

$$F_{rep2} = \frac{n}{2}\eta_j \left(\frac{1}{\rho} - \frac{1}{\rho_0}\right)^2 \frac{\rho_g^{n-1}}{(1+\rho_g^n)^2} \tag{12}$$

draws the robot to the goal.

Fig. 1 shows the attractive and repulsive AAPF force components. The total force generated from the AAPF guides the robot end effector to the goal, represented by the green circumference. For this method to work in real situations, the shape of the object must be filled with spheres representing repulsive fields, as shown in Fig. 3.

So that only the end effector, and not the other links, can reach a position within the obstacle's field of influence, AAPFs were applied only to the last link, while the other links remain using the APFs. This ensures that the other links do not enter the obstacle's influence area.

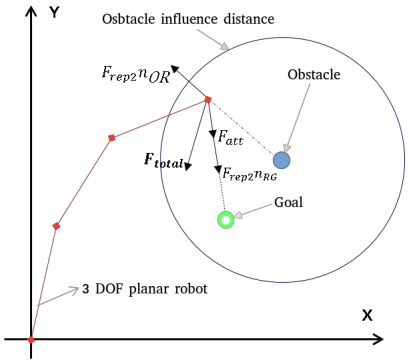

Fig. 1. AAPF attractive and repulsive force components.

4. ORIENTATION CONTROL

The APF was also implemented in configuration space in order to control the orientation of the end effector through all the trajectory. The initial end effector orientation q, corresponding to Roll, Pitch and Yaw angles, is set equal to the grasping orientation q_{final} for the robot to keep current set orientation while it is moving. The attractive force in configuration space is given by

$$\begin{aligned} F_{att_\omega}(q) &= -\nabla U_{att}(q) \\ &= \begin{cases} -\zeta(q - q_{final}) & ; \quad \rho_f(q) \le d \\ \dfrac{-d\zeta(q - q_{final})}{\rho_f(q)} & ; \quad \rho_f(q) > d \end{cases} \end{aligned} \tag{13}$$

where $\rho_f(q)$ is the distance from q to q_{final} and d is defined as the influence distance to the final orientation in radians. Fig. 2 shows the UR5 base link frame and the end effector frame. The axis x_i, y_i and z_i of the end effector frame f_{r_2} gets attracted by the axis x_{i-1}, y_{i-1} and z_{i-1} of the UR5 base link frame f_{r_1} in configuration space.

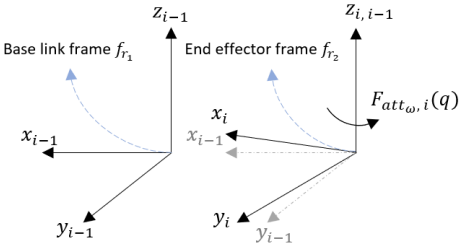

Fig. 2. Reference frame of the UR5 base link and end effector.

To implement the end effector orientation control, the Jacobian matrix was divided into linear Jacobian J_v (the submatrix formed by the three first rows of the Jacobian matrix) and angular Jacobian J_ω (the submatrix formed by the three last rows of the Jacobian matrix), each one having $3 \times c$ dimension (for this work, $c = 6$ and the control points are the UR5 joints), as described in (14).

$$J_{c\times c} = \begin{bmatrix} J_{v3\times c} \\ J_{\omega 3\times c} \end{bmatrix} \tag{14}$$

The attractive forces of each control point i in configuration space are transformed into joint torque through the transposed angular Jacobian $J^T_{\omega,i}$, where J_i is the Jacobian matrix from the base frame to the i^{th} joint. The total artificial joint torque acting on the arm is defined as:

$$\tau(q) = F_{\omega,i}(q) + F_{v,i}(q) = \sum_i J^T_{\omega,i}(q) F_{att_\omega}(q) + \sum_i J^T_{v,i}(q) F_{att,i}(q) + \sum_i J^T_{v,i}(q) F_{rep,i}(q) \quad (15)$$

where, i represents the i^{th} joint. The force $F_{\omega,i}(q)$ is equivalent to the attractive force in configuration space imposed to the joints, so the end effector's orientation keeps constant, and $F_{v,i}(q)$ is the resulting force in the workspace.

5. EXPERIMENTAL RESULTS

The problem domain comprises an additive manufacturing process, where a part will be produced in a 3D printer, then the robot must reach the 3D printer in a specific orientation, grasp the part and carry it to a defined location. The manipulator used is a UR5 robotic arm, from Universal Robots. It has 6 degrees of freedom, a maximum payload of 5 kg and weights 20,6 kg (Robots, 2019).

Three experiments were done in the same environment, the first and second ones using the AAPF and APF with orientation control, respectively, and the third one using the AAPF without orientation control. The task was to approach an object inside a 3D printer with a very narrow opening in the front side. The printer was modelled as a set of spherical obstacles, twelve points for the front side and one point for the tray, as shown in Fig. 3, where the obstacles are the red spheres. As the space in the print area is narrow, and the object to approach is small, the tray was modelled as a bigger sphere involving the object to be picked. This way, the attractive force from the goal won't drag the end effector in the tray's direction.

Aiming to make the approach in a good configuration so the end effector can easily enter the printer and reach the objective, the orientation control method was applied to guarantee the correct final pose of the planned path. The AAPF method was applied only to the tray obstacle to avoid collisions with the outer parts of the printer. Thus the other obstacles repulsive forces stay the same as the classic APF. Similarly, to avoid collisions with the manipulator's links, the AAPF method was applied only to the grasping control point. Therefore, the other control points will never try to enter an obstacle influence area. These considerations make the technique application less likely to cause accidental collisions in the printer inner area.

From Fig. 4 one can see that the beginning of the three paths is identical (the part where the distance is superior to around $0.3m$). That is the obstacle-free part of the planned path. This is so because when the manipulator is relatively far from the obstacles, the resulting force of the AAPF method becomes equal to the one from the APF method, as expected. In the areas near the obstacles, the differences begin to be relevant, and the paths differ from each other.

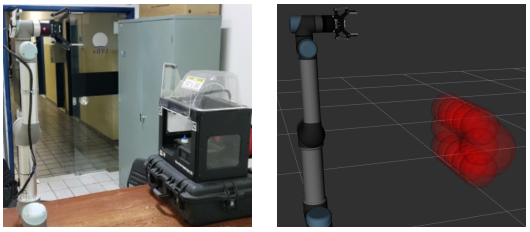

(a) Real model (b) Virtual environment

Fig. 3. Experiment arrange showing (a) the UR5 manipulator, the 3D printer and (b) the simulated environment.

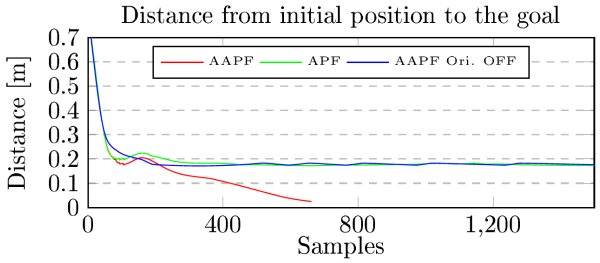

Fig. 4. Comparison of the distance from UR5 end effector to the goal using APF and AAPF with orientation control and AAPF without orientation control

Also, from Fig. 4 is possible to see that the AAPF method with orientation control is the only method that converges to the goal. Although the AAPF without orientation control is still better than the APF with orientation control as it can enter the repulsive fields, the uncertainty of the tool orientation when approaching the printer narrow opening makes this method unreliable to achieve the goal as it is susceptible to other local minimum problems than GNRON. This shows the importance of orientation control in cases like this.

Fig. 5 and Fig. 6 show that the only case where both attractive and repulsive forces go to zero is the AAPF with orientation control method, proofing its convergence. For the APF method, the repulsive force presents a wobbling behaviour leading to an unstable situation, because the limitation of this method to handle the GNRON problem and interact well with several obstacles in a narrow area. In the AAPF without orientation control case, the repulsive force stabilizes in a non-zero value, characterizing a local minimum caused due to the bad final position of the planning solution. The abrupt changes in the magnitudes of force are due to the entry of the end effector into the repulsive fields.

Fig. 7 shows the paths in configuration space. Note that in Fig. 8 the robot adjusts its orientation as it reaches the final position, grasping the object correctly. In Fig. 9 it is shown that, although using the AAPF method, the robot stagnates and oscillates because its actual orientation does not allow to enter potential repulsive fields. Fig. 10 shows that, even though the orientation control method was applied to the classic APF method, it was not possible to reach the goal due to GNRON problems. Note that only the AAPF method with orientation control reaches the goal, while the other methods stopped by the maximum sample number condition. The technique presented similar performance to the simulated environment in the real

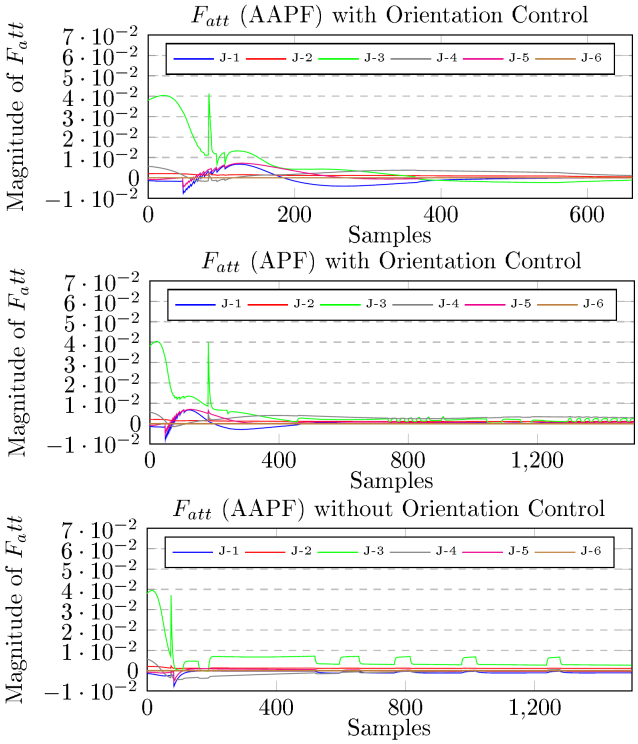

Fig. 5. Comparison between attractive forces using AAPF and APF with orientation control and AAPF without orientation control

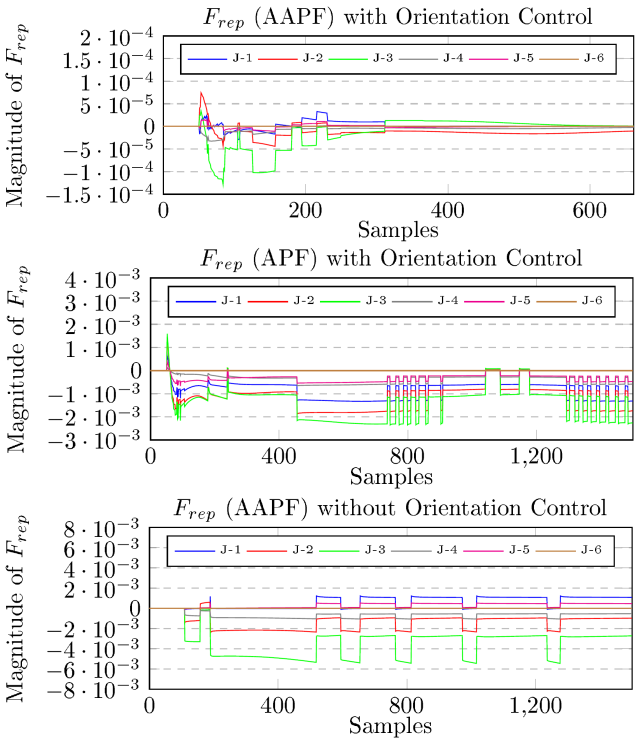

Fig. 6. Comparison between repulsive forces using AAPF and APF with orientation control and AAPF without orientation control

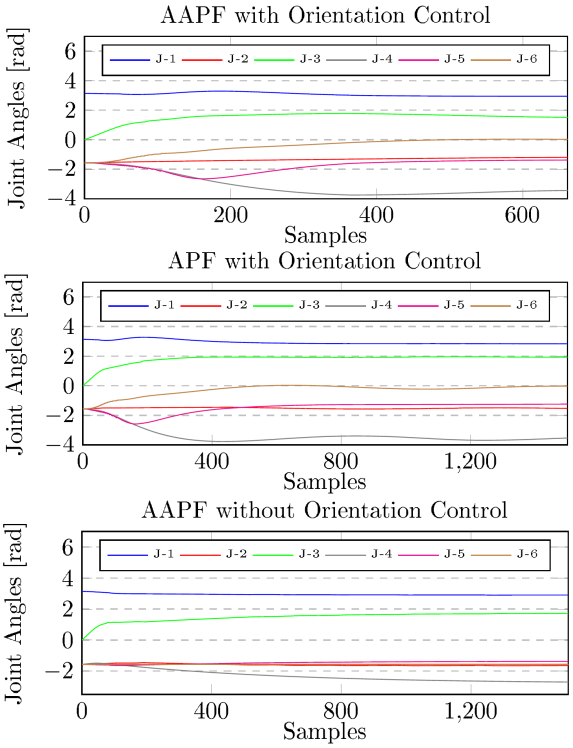

Fig. 7. Comparison between UR5 joint angles using AAPF and APF with orientation control and AAPF without orientation control

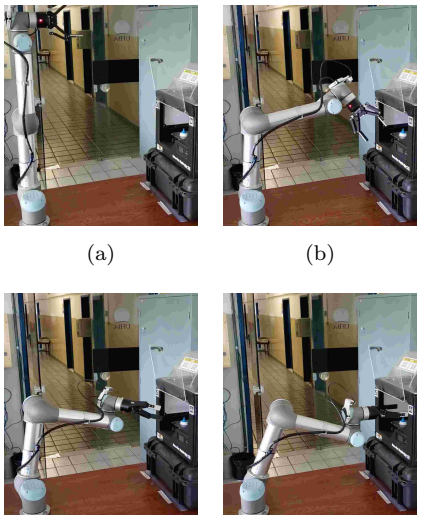

Fig. 8. AAPF with orientation control method applied on real scenario

hardware. The video showing the experiments is available at `https://youtu.be/9d7lBqTH_JA`.

6. CONCLUSIONS

In this paper, we introduced a new end effector orientation control technique which allows reaching a desired end effector orientation using AAPF. The local minimum known as GNRON problem was avoided using of the AAPF method. It was shown that the use of this method reduces the jitter in narrow areas and allow the end effector to reach the goal even if it is inside the obstacle influence area. Experimen-

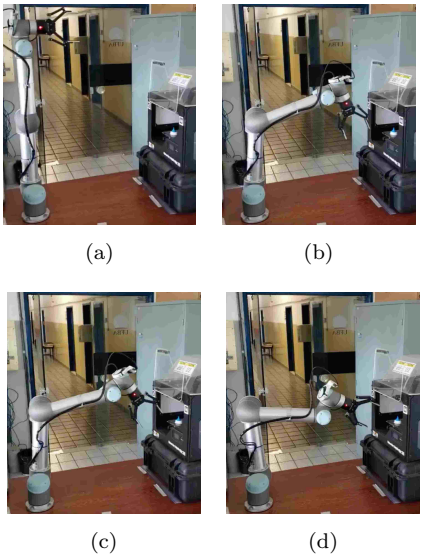

(a) (b) (c) (d)

Fig. 9. AAPF without orientation control method applied on a real scenario

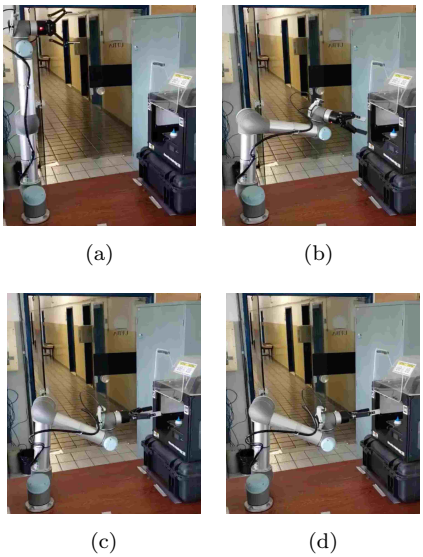

(a) (b) (c) (d)

Fig. 10. APF with orientation control method applied on a real scenario

tal results of the AAPF method used with the proposed orientation control technique perform as expected by the theory.

Despite the results, the manipulator not always reaches the goal due to the static weights for the attractive and repulsive forces. It is necessary to update them constantly, so a balance in the potential fields is achieved. In future works, a method for environment exploration with autonomous goals and obstacles recognition with computer vision will also be implemented.

ACKNOWLEDGEMENTS

This study has received funding from SEPIN/MCTI under the 4 th Coordinated Call BR-EU in CIT and from the European Unions Horizon 2020 research and innovation programme under the Grant Agreement No 777096. The authors thank FAPESB (Fundação de Amparo à Pesquisa do Estado da Bahia) for their financial support.

This study was financed in part by the Coordenação de Aperfeiçoamento de Pessoal de Nível Superior - Brasil (CAPES) - Finance Code 001.

REFERENCES

Akbaripour, H. and Masehian, E. (2017). Semi-lazy probabilistic roadmap: a parameter-tuned, resilient and robust path planning method for manipulator robots. *The International Journal of Advanced Manufacturing Technology*, 89(5-8), 1401–1430.

Byrne, S., Naeem, W., and Ferguson, S. (2013). An intelligent configuration-sampling based local motion planner for robotic manipulators. In *9th International Workshop on Robot Motion and Control*, 147–153. IEEE.

Ge, S.S. and Cui, Y.J. (2000). New potential functions for mobile robot path planning. *IEEE Transactions on robotics and automation*, 16(5), 615–620.

Khatib, O. (1986). Real-time obstacle avoidance for manipulators and mobile robots. In *Autonomous robot vehicles*, 396–404. Springer.

Kim, Y.H., Son, W.S., Park, J.B., and Yoon, T.S. (2016). Smooth path planning by fusion of artificial potential field method and collision cone approach. In *MATEC Web of Conferences*, volume 75, 05004. EDP Sciences.

Leite, A.C., Almeida-Antonio, T.B., From, P.J., Lizarralde, F., and Hsu, L. (2015). Control and obstacle collision avoidance method applied to human-robot interaction. In *2015 IEEE International Workshop on Advanced Robotics and its Social Impacts (ARSO)*, 1–8. IEEE.

Li, G., Tong, S., Cong, F., Yamashita, A., and Asama, H. (2015). Improved artificial potential field-based simultaneous forward search method for robot path planning in complex environment. In *2015 IEEE/SICE International Symposium on System Integration (SII)*, 760–765. IEEE.

Luo, J., Su, W., and Wang, D. (2012). The improvement of the artificial potential field robot path planning based on 3-d space. In *International Conference on Automatic Control and Artificial Intelligence (ACAI 2012)*, 2128–2131. IET.

Quiroz-Omaña, J.J. and Adorno, B.V. (2019). Whole-body control with (self) collision avoidance using vector field inequalities. *IEEE Robotics and Automation Letters*, 4(4), 4048–4053. doi:10.1109/LRA.2019.2928783.

Robots, U. (2019). Ur5 collaborative robot arm — flexible and lightweight robot arm. `https://www.universal-robots.com/products/ur5-robot/`. Accessed: 2019-10-15.

Thomas, C., Busch, F., Kuhlenkoetter, B., and Deuse, J. (2011). Process and human safety in human-robot-interaction-a hybrid assistance system for welding applications. In *International Conference on Intelligent Robotics and Applications*, 112–121. Springer.

Zhang, Y., Liu, Z., and Chang, L. (2017). A new adaptive artificial potential field and rolling window method for mobile robot path planning. In *2017 29th Chinese Control And Decision Conference (CCDC)*, 7144–7148. IEEE.